Crosscorrelation to Velocity Calibration: Automated detection of perforation signals and multi-stage velocity model inversion in microseismic monitoring

Fernando Castellanos[1], Mike Preiksaitis[1], Vlad Shumila, Ryan Nader[1], Doug Angus[1]

1 – ESG Solutions

Summary

Using different datasets, we showcase an automated workflow for identifying perforation (perf) shots and subsequently inverting to calibrate Velocity Models (VMs) using Particle Swarm Optimization (PSO) in order to efficiently and accurately locate microseismic events. First, we show that perf signals can be discriminated from other triggers using crosscorrelation (CC) methods and hodogram analysis. Next, we use these identified perfs and group them along sections of the well to construct well-constrained VMs based on quantitative and objective attributes. With an example dataset, we demonstrate an automated approach that allows a threefold improvement (two days) in elapsed processing time when compared to using a standard approach (six days).

Theory / Method

Automatic Perf Detection using CC

CC techniques have been used to detect repeating microseismic events, known as multiplets (Arrowsmith and Eisner, 2006; De Meersman et al., 2009; Castellanos and Van der Baan, 2015; Jones et al., 2014). The assumption is that these events come from the same source area, traveling with similar ray paths, and so they are expected to have nearly-identical waveforms. Similarly, we can assume that perfs from the same hydraulic fracturing stage share similar waveforms, i.e., the perfs exhibit high correlation with other perfs, while sharing dissimilar characteristics, i.e., low correlation, to that of any other microseismic events. Preliminary studies by Castellanos et al. (2019) found this perf similarity approach successfully detected most perfs in a dataset. In our automated workflow, we perform the following steps: 1) for each individual stage we select all the triggers recorded during perf times (usually a 5-10 minutes time span when they are detonated); 2) for each trigger pair combination, we extract a time window of data around autopicked P-waves and compute a weighted average of the CC coefficients across all sensors; 3) we create an upper triangular matrix containing the CC coefficients of all pair permutations; and 4) a minimum CC threshold is set, which allows identifying the group of highly correlated triggers, most likely the perfs. However, when more than one group is found, which is common in simultaneous frac treatment or due to the triggering of nearby microseismic activity, we add a fifth step, where we use particle motion analysis (e.g., Montalbetti and Kanasewich, 1970) to identify the group whose back-azimuths point towards the stage zone centroid.

Figure *1* compares the waveforms from a perf and a typical microseismic event. The event on the right shows the arrival of the P-wave followed by a higher-amplitude S-wave, whereas the perf (on the left) shows a strong P-wave arrival followed by a lower amplitude S-wave. There are also differences in the frequency content. These two triggers belong to two different clusters (or groups) of highly similar triggers. When plotting the particle motion vectors (or back azimuths) of all triggers within each detected cluster, we observe that the perf cluster point towards the perf zone whereas the microseismic events do not.

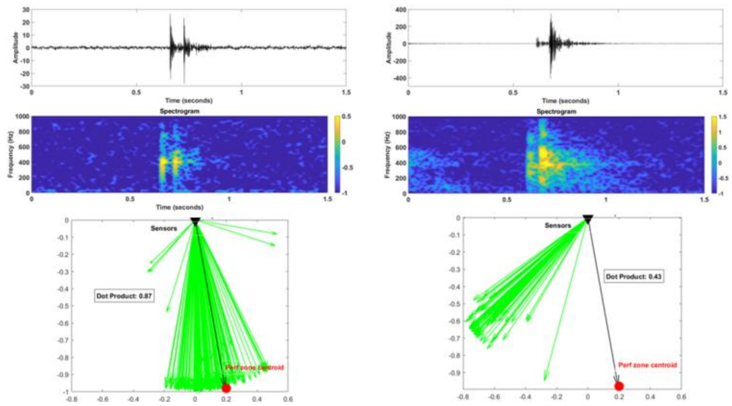

Figure 1. Top: Waveforms and spectrograms from two different clusters recorded during expected perf times. Bottom: Corresponding particle motions from the two clusters detected within the perf time window. By comparing particle motion (green arrows) and perf zone-sensor angles via dot product, we can find which cluster most likely contains the perf waveforms.

PSO-based Velocity model Inversion

For VM inversion we apply PSO, a population-based stochastic optimization technique, using data with known locations (perf shots, string shots) and early-stage microseismic events (Clerc and Kennedy 2002; Urbancic et al., 2006). By varying the target function and imposed constraints, PSO can generate VM solutions suitable for a space and time-evolving rock mass and multiple monitoring array configurations. Since using a single VM for the entire treatment well may not be suitable due to variable local velocity, we allow for VM variations across defined sections, here called “checkpoints”, along the well (e.g., heel, mid-lateral, toe). This allows the automated inversion approach to develop a discrete (or blocky) two-dimensional VM. For short wells (lengths < 2 km) with limited structural changes, two or three sections or “checkpoints” per well may be enough, whereas for longer wells (lengths> 2 km), with more variable structure, a higher number of sections are likely required.

For each checkpoint, a quantitative criterion is used to identify the optimal solution. This requires: 1) balancing the desire to minimize the residuals (observed vs modelled travel times) and 2) ensuring that velocity variations follow impedance contrasts range within the geological medium

Results, Observations

We apply the perf detection methodology on a test dataset with 21 stages. We successfully detected 138 out of 139 perfs (99% success rate) and with a single false positive. Figure 2 shows upper triangular CC matrices for all triggers (310 in total) recorded during perf times of five consecutive stages (out of 21). In Figure 2a, we apply an appropriate time window that encompasses the signals, and as a result, clusters of highly correlated triggers (perfs) are clearly visible. In Figure 2b, a very short time window for CC analysis was used, resulting in high crosscorrelation values due to the influence of individual periods of seismic signal and not the average seismic signal. Using a CC threshold of 0.8 is sufficient to correctly gather all the perfs into one group (Figure 2a) without any false positives, whereas a shorter time window gathers into one group all the perfs but also an additional 158 false positives.

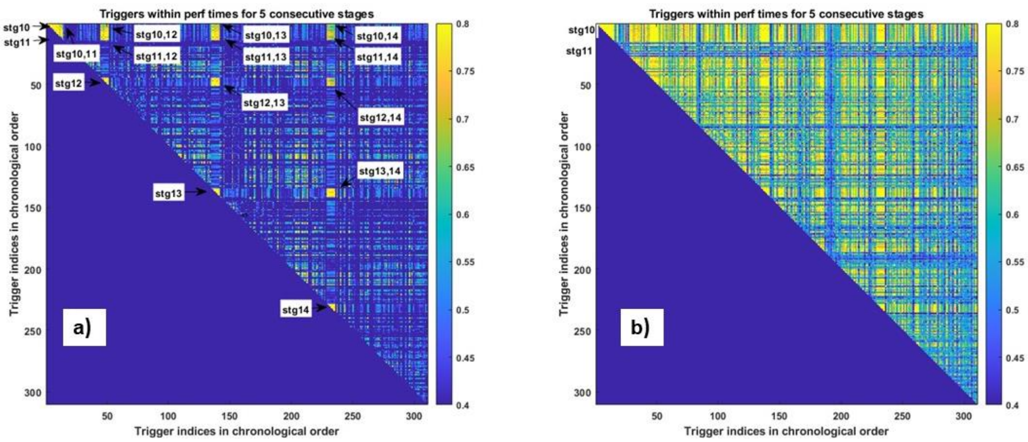

Figure 2. Upper-triangular CC matrix for all triggers (310 in total) recorded during perf time windows of five consecutive stages: (a) an appropriate time window length of 26 ms with a 0.8 CC threshold detects all perfs with no false positives and (b) a very short time window was used that results in distorting CC values.

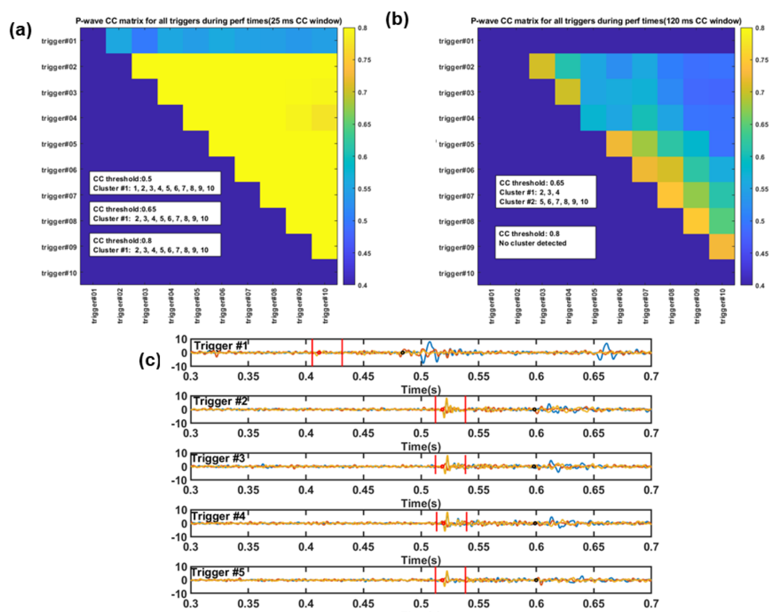

Figure 3. Effect of different time window lengths and minimum CC threshold on the detection of clusters containing perfs: (a) 25 ms time window, (b) 120 ms time window and (c) waveforms of the first five triggers recorded at the same sensor.

Figure 3 shows the effect of different time window lengths and CC threshold on perf detection. Here we use triggers recorded during perf time windows for one stage from a second example dataset. In Figure 3a, an ideal window length (mostly P-wave signal) and CC threshold greater than 0.65 allows for proper discrimination between a non-perf (trigger #1) and actual perfs (triggers #2 to #9). In Figure 3b, a longer window is used that includes noise, thus reducing the overall CC levels. This prevents the detection of all the perfs within the same cluster. Figure 3c shows waveforms from the first five triggers recorded at the same sensor, where we clearly observe the waveforms of the first trigger (non-perf) differs from the rest (perfs).

PSO-based Velocity model Inversion

We apply the automated PSO-based VM inversion on a dataset consisting of three vertical receiver arrays to monitor microseismicity from a stimulation targeting the Wolfcamp and Spraberry formations in the Permian Basin. Figure 4 shows the perf location results and histogram that reveal most perfs locate within 30 ft from their expected known locations. This provides confidence in the use of the PSO-based VMs along the different sections of the treatment well to subsequently locate MS events.

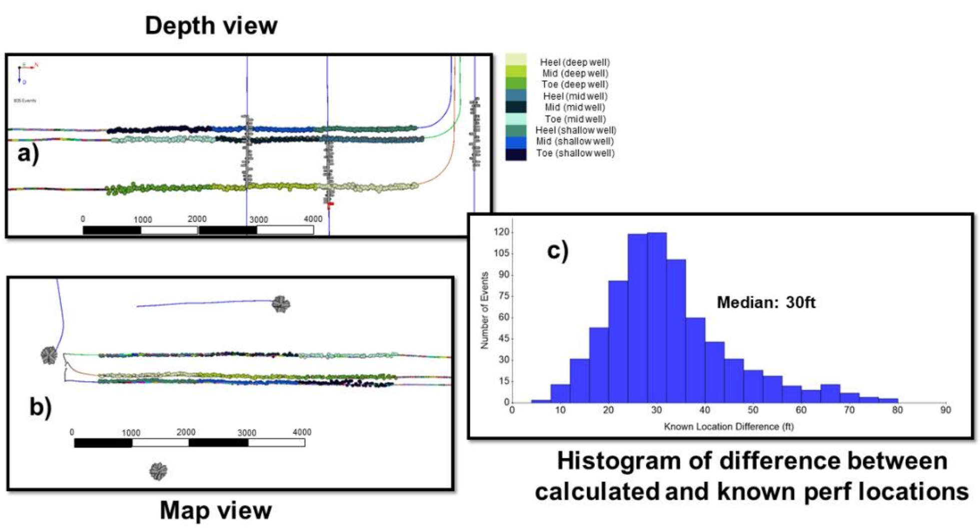

Figure 4. Perf location results (color-scaled by checkpoint) after PSO-based velocity model inversion: (a) depth view, (b) map view and (c) histogram of perf location difference (calculated vs known).

We apply the automated PSO-based VM inversion on a second dataset, where a conventional vertical receiver array monitors microseismicity from a stimulation targeting a formation in the Western Canadian Sedimentary Basin. In previous work (Castellanos et al, 2019), we assess different scenarios and show why a single PSO VM is not adequate to locate all perfs close to their expected locations, and the need for slightly varying VMs. Figure 5 shows the resulting microseismic locations using the automated approach (Figure 5c,5d,5e) are consistent with the standard approach (Figure 5a, 5b)., For most perfs in this dataset, the automated PSO algorithm finds a best-fitting model with location difference less than 25 m. Furthermore, the constrained PSO algorithm generally only deviates from well log determined velocities on the order of ±5% with respect to the P- and S-wave velocities and on the order of ±10% for anisotropy.

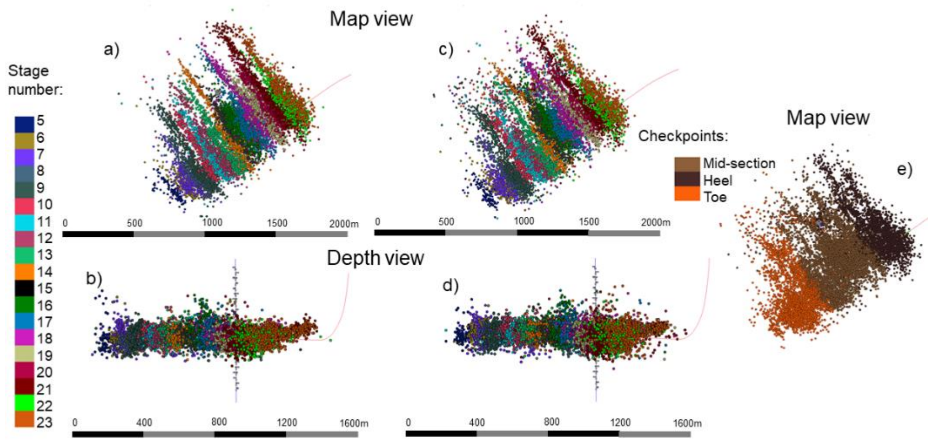

Figure 5. Microseismic event locations are shown for the standard approach in map view (a) and depth view (b) and the automated approach in map view (c) and depth view (d). The events are coloured by stage in (a)-(d) and coloured by PSO checkpoint VM in (e).

Discussion/Conclusions

We have shown an innovative approach consisting of integrating the perf detection using cross-correlation and velocity model optimization using PSO to provide a scalable robust workflow for microseismic calibration. This allows for a fast and quantitative assessment of optimal velocity models at different sections along the treatment well, aimed at significantly reducing the time an analyst would need to visually inspect potential perfs and apply QC measures to finalized velocity models. We recommend prior noise attenuation on perfs since low SNR data would require lower cross-correlation thresholds (<0.8), resulting in undesired false positives. As for PSO inversion, prior site information such as sonic and other logs, anisotropy, formation tops, presence of adjacent wells, are key to evaluating and constraining a feasible range of velocity perturbations to find optimal velocity models.

References

Arrowsmith, S. J., and Eisner, L., 2006, A technique for identifying microseismic multiplets and application to the Valhall Field, North Sea. Geophysics, 71 (2), V31–V40.

Castellanos, F., and Van der Baan, M., 2015, Waveform similarity for quality control of event locations, time picking and moment tensor solutions. Geophysics, 80 (6), WC99-WC106.

Castellanos, F., Preiksaitis, M., Nader, R., Shumila, V., Falls, S., Hook, D., Angus, D., 2019, An automated quantitative multi-stage approach to invert velocity models for microseismic event locations, First Break, 37, 61-67.

Clerc M. and Kennedy, J., 2002, The Particle Swarm-Explosion, Stability, and Convergence in a Multidimensional Complex Space. IEEE Transactions on Evolutionary Computation, 6, 58-73

De Meersman K., Kendall J.-M. and Van der Baan M., 2009, The 1998 Valhall microseismic data set: An integrated study of relocated sources, seismic multiplets and S-wave splitting. Geophysics 74, B183–B195.

Jones GA, Kendall JM, Bastow ID, Raymer DG, Wuestefeld A., 2014, Characterization of fractures and faults: a multi-component passive microseismic study from the Ekofsk reservoir. Geophys Prospect 62:779–796.

Montalbetti, J.M. and Kanasewich, E.R., 1970, Enhancement of teleseismic body phases with a polarization filter. Geophys. J. R. astr. Soc., 21, 119–129

Urbancic, T. Zantout, S. and McGillivray, P., 2006, Simultaneous inversion for velocity and passive microseismic event locations: a particle swarm optimization approach. First EAGE Passive Seismic Workshop - Exploration and Monitoring Applications, Extended Abstracts